NeuroImage

www.elsevier.com/locate/ynimg
NeuroImage 35 (2007) 1028–1037

Identifying patients with obsessive–compulsive disorder using whole-brain anatomy

Carles Soriano-Mas,[a,*] Jesús Pujol,[a] Pino Alonso,[b] Narcís Cardoner,[b] José M. Menchón,[b] Ben J. Harrison,[a,c] Joan Deus,[a,d] Julio Vallejo,[b] and Christian Gaser[e]

[a]*Institut d'Alta Tecnologia (IAT)-PRBB, CRC Corporació Sanitària, Passeig Marítim 25-29, Barcelona 08003, Spain*
[b]*Department of Psychiatry, Hospital of Bellvitge, University of Barcelona, Spain*
[c]*Melbourne Neuropsychiatry Centre, Department of Psychiatry, The University of Melbourne, Australia*
[d]*Department of Clinical and Health Psychology, Autonomous University of Barcelona, Spain*
[e]*Department of Psychiatry, University of Jena, Germany*

Received 23 November 2006; revised 12 January 2007; accepted 16 January 2007
Available online 27 January 2007

Structural neuroimaging studies have reported a variety of brain alterations between groups of obsessive–compulsive disorder (OCD) patients and healthy controls. However, the large heterogeneity in discrete anatomical measures that exists among patients prevents a clear discrimination of single patients from healthy subjects. This reduces the potential clinical applicability of structural neuroimaging studies. In the present study we assessed the feasibility of identifying OCD patients on the basis of whole-brain anatomical alterations. Whole-brain magnetic resonance images were collected from two consecutive samples of OCD outpatients ($n=72$ and $n=30$), and control subjects ($n=72$ and $n=30$). We computed the whole-brain (voxel-wise) pattern of structural difference between OCD patients and control subjects at the group level. A single expression value of this difference pattern was calculated for each subject, expressing their degree of 'OCD-like' anatomical alteration. Accuracy of patient classification based on these expression values was assessed using two validation approaches. Firstly, using a cross-validation method, we obtained a high classification accuracy (average of the sensitivity and specificity indices) of 93.1%. In a second assessment, which classified new groups of OCD patients and control subjects, overall accuracy was lower at 76.6%. Individual expression values for OCD patients were significantly correlated with overall symptom severity as measured by the Y-BOCS scale. Our results suggest that OCD patients can be identified on the basis of whole-brain structural alterations, although the accuracy of our approach may be limited by the inherent variability of psychiatric populations. Nevertheless, the anatomical characterization of individual patients may ultimately provide the psychiatrist with relevant biological information.

Introduction

Reports of altered brain structure are common in magnetic resonance imaging (MRI) studies of obsessive–compulsive disorder (OCD) (Rauch and Baxter, 1998; Saxena et al., 1998). Although some variability exists among studies focusing on particular regions of interest (ROIs), including several null reports (Aylward et al., 1996; Bartha et al., 1998; Kellner et al., 1991; Riffkin et al., 2005; Stein et al., 1997), significant volumetric alterations have been described in different cortical and subcortical structures, such as the basal ganglia (Giedd et al., 2000; Robinson et al., 1995; Rosenberg et al., 1997; Scarone et al., 1992; Szeszko et al., 2004a), thalamus (Atmaca et al., 2006; Gilbert et al., 2000), orbitofrontal cortex (Atmaca et al., 2006; Choi et al., 2004; Kang et al., 2004; Szeszko et al., 1999), amygdala (Kwon et al., 2003; Szeszko et al., 1999, 2004b), or the cerebellum (Jenike et al., 1996). Importantly, this wide distribution of volumetric changes described by ROI studies has since been confirmed in studies using voxel-based morphometry (VBM) (Kim et al., 2001; Pujol et al., 2004; Valente et al., 2005), a structural MRI analysis technique that permits systematic assessments of the entire brain on a voxel-by-voxel basis (Ashburner and Friston, 2000). Since VBM studies, by virtue of their automated nature, can facilitate assessments of large MRI series of patients and control subjects, they appear to be more suitable for characterizing structural brain anomalies occurring with the highest prevalence in OCD patients (Pujol et al., 2004).

Despite the increasing interest in volumetric MRI studies of psychiatric patients, it is important to recognize that neither analysis approach described above, ROI or VBM, is intended as a patient classification or diagnostic tool, as they describe anatomical differences which are suitable for interpretations at the group, or population, level (Friston and Ashburner, 2004). Identification of gross anatomical anomalies in specific patients is uncommon, and typically a large overlap exists between patient and control groups in each discrete (e.g., voxel-by-voxel) anatomical measure (Davatzi-

* Corresponding author. Fax: +34 93 221 6818.
E-mail address: csoriano@crccorp.es (C. Soriano-Mas).
Available online on ScienceDirect (www.sciencedirect.com).

1053-8119/$ - see front matter © 2007 Elsevier Inc. All rights reserved.
doi:10.1016/j.neuroimage.2007.01.011

kos, 2004). As a consequence, the information obtained from neuroimaging studies is rarely used in a clinical context and contributes little to patient management. Nevertheless, it is possible that a clearer discrimination between groups may be obtained if analyses were not based on discrete anatomical measurements, but rather, on the whole-brain pattern of abnormalities. Such a method could ultimately provide the clinician with the opportunity of classifying subjects on the basis of a relevant (anatomically informed) source of information.

The aim of this study was to assess the feasibility of classifying single subject cases of MRI data as OCD patients or healthy controls using their whole-brain anatomy. Specifically, we sought to characterize each subject with a single value that reflected the extent of expression of the whole-brain pattern of anatomical abnormalities depicted by the OCD group. This pattern was computed through an optimized VBM analysis of our large MRI series of OCD patients and matched control subjects (Pujol et al., 2004). The accuracy of this classification approach was then evaluated by using a cross-validation method, and also with an independent set of data of newly recruited OCD patients and control subjects.

Materials and methods

Subjects

In total, 204 subjects were included in the study. An initial sample of 72 OCD patients and 72 control subjects was used to develop the whole-brain classification scheme that will be detailed below. This sample, referred to here as the original sample, has been previously described (Pujol et al., 2004), and included OCD patients and control subjects who were matched for age, gender and handedness. In the current study, we also recruited a second (new) sample of 30 OCD patients and 30 control subjects. Subjects from both OCD subgroups were community outpatients consecutively recruited when two psychiatrists (P.A. and J.M.M.), who independently assessed the patients, agreed on their diagnosis. Exclusion criteria included a history of relevant medical illness, or any neurological or other psychiatric diseases. No patient met the criteria for Tourette's syndrome or had a recent history of psychoactive drug use/abuse. Comorbid anxious and depressive symptoms were not considered as an exclusion criterion, provided that OCD was the primary clinical diagnosis. Table 1 summarizes the sociodemographic characteristics of the two study samples, and Table 2 presents the primary clinical features of OCD patients. All subjects gave written informed consent to participate in this study, following a complete description of the protocol, which was approved by the Institutional Review Board of the University Hospital of Bellvitge, Barcelona.

MRI acquisition and processing

A 1.5-T magnet (Signa, GE Medical Systems, Milwaukee, WI) was used to obtain a sixty-slice 3D spoiled gradient-recalled acquisition sequence in the sagittal plane (TR 40 ms, TE 4 ms, pulse angle 30°, field of view 26 cm, matrix size 256 × 192 pixels, and section thickness between 2.4 and 2.6 mm). Imaging data were then transferred and processed on a Microsoft Windows platform running MATLAB version 6.5 (The MathWorks Inc., Natick, MA) and Statistical Parametric Mapping software (SPM2; The Wellcome Department of Imaging Neuroscience, London, England). Image preprocessing was based on the optimized procedure for structural neuroimaging data (including the creation of a customized template) (Good et al., 2001), which was automated with two freely available MATLAB scripts (cg_create_template and cg_vbm_optimized, see http://www.dbm.neuro.uni-jena.de/vbm/). After tissue segmentation, we focused our whole-brain structural imaging analysis on subjects' segmented gray matter volumes, informed by our previous results (Pujol et al., 2004). Importantly, in order to preserve volumetric information, the last step of the preprocessing consisted in the modulation of voxel values by the Jacobian determinants derived from the normalization step. All resulting gray matter volumes were then smoothed with a small isotropic kernel of 4 mm (Salmond et al., 2002). Final voxel values ranged between 0 and 1. A detailed description of the procedure can be found elsewhere (Pujol et al., 2004).

Statistical analyses

Calculation of the whole-brain pattern of differences and individual expression values

Neuroimaging studies using whole-brain patterns of between-group differences for patient classification purposes have normally used multivariate statistical methods based on Singular Value Decomposition (SVD) for pattern characterization (Kawasaki et al., 2007; Kerrouche et al., 2006; Meyer-Lindenberg et al., 2001; Scarmeas et al., 2004). However, in the case of a single comparison between two groups, as in the present study, the pattern of whole-brain differences characterized with a univariate approach (and its statistical significance), is identical to the one obtained with

Table 1
Sociodemographic characteristics of the study samples

Sociodemographic variable[a]	Original sample		Newly recruited sample	
	OCD (n=72)	Controls (n=72)	OCD (n=30)	Controls (n=30)
	Mean (SD), range	Mean (SD), range	Mean (SD), range	Mean (SD), range
Age (years)	29.8 (10.5), 18–60	30.1 (10.2), 18–57	31.9 (9.3), 18–63	31.8 (10.2), 18–63
Education (years)	13.2 (3.6), 8–17	14.0 (3.1), 8–17	12.2 (2.9), 5–17	13.1 (3.2), 8–17
	N (%)	N (%)	N (%)	N (%)
Gender distribution (females)	32 (45.7)	32 (45.7)	9 (30.0)	14 (46.7)
Handedness (lefthanders)	11 (15.3)	11 (15.3)	2 (6.7)	3 (10.0)

OCD, obsessive–compulsive disorder.
[a] No significant differences were observed between groups in any of the variables.

Table 2
Clinical characteristics of the OCD patients

Clinical variable	Original sample ($n=72$)			Newly recruited sample ($n=30$)			Statistical value [a] (P value [b])
	Mean (SD), range			Mean (SD), range			
Age at onset of OCD (years)	17.0 (5.9), 6–40			19.7 (6.1), 7–36			2.35 (0.03)
Duration of illness (years)	13.0 (10.5), 1–51			11.3 (9.4), 1–39			−0.99 (0.33)
Y-BOCS score (global)	26.7 (7.1), 7–38			21.0 (5.7), 10–32			−5.44 (<0.001)
Y-BOCS score (obsessions)	13.7 (3.4), 6–19			10.9 (3.1), 6–17			−5.02 (<0.001)
Y-BOCS score (compulsions)	13.0 (4.8), 0–19			10.1 (3.0), 1–16			−5.25 (<0.001)
OCD symptoms [c]	0 (Absent)	1 (Mild)	2 (Prom)	0 (Absent)	1 (Mild)	2 (Prom)	
	N (%)	*N* (%)	*N* (%)	*N* (%)	*N* (%)	*N* (%)	
Symmetry and ordering	50 (69.4)	12 (16.7)	10 (13.9)	20 (66.7)	1 (3.3)	9 (30.0)	8.84 (0.01)
Hoarding	56 (77.8)	11 (15.3)	5 (6.9)	15 (50.0)	10 (33.3)	5 (16.7)	13.50 (0.001)
Contamination and cleaning	41 (56.9)	14 (19.4)	17 (23.6)	16 (53.3)	5 (16.7)	9 (30.0)	0.70 (0.70)
Aggressive and checking	23 (31.9)	19 (26.4)	30 (41.7)	6 (20.0)	8 (26.7)	16 (53.3)	2.31 (0.32)
Sexual and religious obsessions	55 (76.4)	4 (5.6)	13 (18.1)	23 (76.7)	3 (10.0)	4 (13.3)	1.41 (0.49)
Comorbid diagnoses	Mean (SD), range			Mean (SD), range			
HAM-D score at inclusion	12.7 (5.4), 2–26			11.9 (5.1), 4–25			−0.88 (0.39)
HAM-A score at inclusion	13.3 (6.6), 0–30			14.5 (4.9), 6–25			1.25 (0.22)
	N (%)			*N* (%)			
Significant history of depression	26 (36.1)			4 (13.3)			6.74 (0.01)
Significant history of anxiety	19 (26.4)			7 (23.3)			0.14 (0.70)
Treatment status	Mean (SD), range (median)			Mean (SD), range (median)			
Cumulative SRIs treatment (months)	41.0 (62.5), 0–396 (24.0)			19.6 (20.5), 0–97 (14.6)			−5.73 (<0.001)
Previous SRI trials completed	*N* (%)			*N* (%)			1.21 (0.75)
Never treated	5 (6.9)			2 (6.7)			…
One SRI trial	19 (26.4)			6 (20.0)			…
Two SRI trials	21 (29.2)			8 (26.7)			…
Three or more SRIs trials	27 (37.5)			14 (46.7)			…
Stable medication at time of the MRI	*N* (%)			*N* (%)			4.05 (0.40)
Medication-free (>4 weeks)	18 (25.0)			4 (13.3)			…
Clomipramine hydrochloride	25 (34.7)			9 (30.0)			…
Fluoxetine or fluvoxamine maleate	13 (18.1)			7 (23.3)			…
Phenelzine sulfate	2 (2.8)			1 (3.3)			…
Clomipramine with fluoxetine	14 (19.4)			9 (30.0)			…

HAM-A, Hamilton Rating Scale for Anxiety.
HAM-D, Hamilton Rating Scale for Depression.
MRI, magnetic resonance imaging.
OCD, obsessive–compulsive disorder.
SRI, serotonin reuptake inhibitors.
Y-BOCS, Yale–Brown Obsessive–Compulsive Scale.
[a] Newly recruited sample compared to (reference) original sample (one-sample t test for continuous variables, χ^2 test for categorical variables).
[b] Two-tailed.
[c] Dimensions from Mataix-Cols et al. (1999). A score of 2 (prominent) was allowed for more than 1 dimension.

multivariate methods based on SVD (Worsley et al., 1997). Consequently, we performed a voxel-wise univariate statistical analysis to characterize the whole-brain pattern of differences between the two study groups.

As depicted in Fig. 1, the method for calculating this whole-brain pattern and individual expression values can be summarized in two basic analysis steps. Firstly, using SPM2, we calculated a whole-brain image of between-group differences (represented by the univariate t statistic) by contrasting, voxel-by-voxel, the preprocessed gray matter volumes of the original sample of 72 OCD patients and 72 control subjects (Fig. 1A). In the second step, this resulting t map was multiplied by the gray matter image of each subject to obtain their individual expression values (Fig. 1B). Both analysis steps are explained in more detail below.

Step 1: Within the general linear model framework implemented in SPM2, we calculated a voxel-wise t statistic image which expressed the areas of significant regional difference in gray matter volume between OCD patients and control subjects. This t statistic map was designed specifically to represent the areas of increase (i.e., positive t values) and decrease (i.e., negative t values) of regional gray matter volume in OCD patients versus control subjects. In the calculation of this difference map, we covaried for subjects' age as a

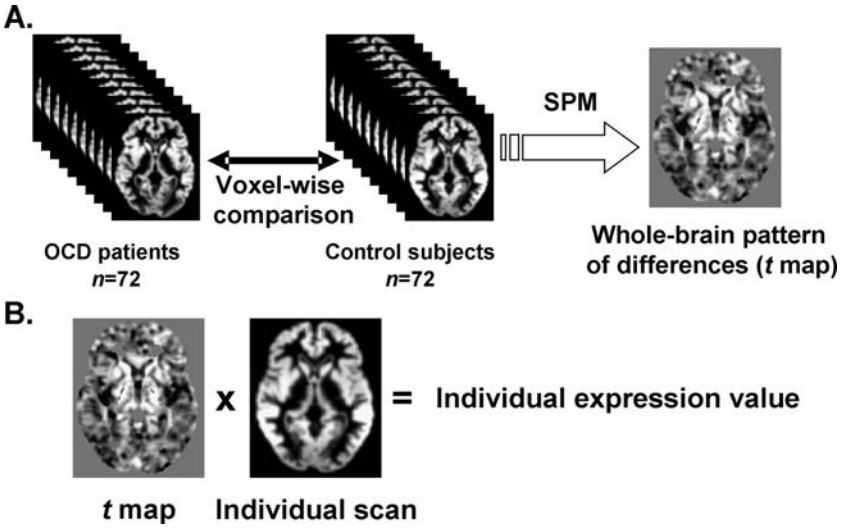

Fig. 1. Schematic illustration of the method developed to obtain the expression values of individual subjects. (A) Calculation of the whole-brain pattern of structural differences between groups. (B) Calculation of individual expression values.

confounding variable. To control for any global differences in gray matter volume, data were proportionally scaled to a grand mean of 100. To assess the global significance of the pattern of differences we used the omnibus mean sum of squares test (Worsley et al., 1995). This can be defined as $S=\sum t^2/N$, where the summation of the square of the t value calculated over all voxels is divided by the total number of voxels N. This test allowed for the rejection of the null hypothesis that no significant between-group differences in entire gray matter volume existed between groups, without localizing such differences. Omnibus significance testing can then be approximated with a χ^2 distribution (Worsley et al., 1995).

Step 2: To obtain each subject's individual expression value of the pattern described above, we individually computed the scalar product of the gray matter image by the t map of between-group differences. That is, we multiplied each voxel of the individual gray matter images by the voxel's relevance in between-group discrimination. These voxel values were then added up, summarizing the anatomical features of each subject into a single value that represented the extent to which they expressed the pattern of anatomical differences characterized at the group level. Subjects showing a large gray matter volume in voxels with positive values in the t map, and relatively small gray matter volume in voxels with negative t values (i.e., OCD patients) were expected to display positive expression values. Conversely, subjects with the inverse pattern of gray matter distribution (i.e., control subjects) were expected to display negative expression values.

Because the current analysis strategy that we used to calculate gray matter volumes differences between OCD patients and control subjects (i.e. *Step 1*) was similar to our previous VBM study of the same subjects (Pujol et al., 2004), we expected strong overlap of the patterns of volumetric differences described in each study (see Results section). The major differences between studies with respect to the new analysis employed here involved the use of SPM2 normalization and segmentation algorithms (versus SPM99), as well as spatial smoothing with a smaller Gaussian kernel (4 mm versus 12 mm), which increased the number of independent elements available for calculating individual expression values. In addition, to satisfy the aims of the new analysis, a single design matrix was constructed, which specified that global gray matter volume was accounted for both in the calculation of volumetric decreases and increases. In the previous study, two design matrices were constructed and global gray matter volume was only controlled in the description of volumetric increases (see Pujol et al., 2004).

Subject classification

To make subject classifications, we first calculated the mean expression value for the two groups of the original sample, OCD patients ($n=72$) and control subjects ($n=72$). Next, we calculated the two distances (Euclidean) between each subject's individual expression value and each group's mean expression value. These two distances were then converted to complementary probabilities of being an OCD patient (P-OCD = 1 − distance to the OCD mean / distance to the OCD mean + distance to the control mean) or a control subject (P-Control = 1 − distance to the control mean / distance to the OCD mean + distance to the control mean). OCD patients were considered to be misclassified when P-OCD was smaller than P-Control, that is, less than 0.5, and vice versa.

We validated our classification approach in two ways. Firstly, we conducted a cross-validation study with the leave-one-out method (a.k.a. jackknife approach). This was performed by omitting one subject at a time from the original study sample and then computing a new t map (*Step 1* above) from the remaining sample (143 subjects). The expression value (*Step 2*) and classification (P-OCD and P-Control) for this left-out-subject were then calculated. This process was repeated 144 times, accounting for all subjects.

Secondly, we performed an 'independent set of data' analysis to evaluate the rate of misclassification of a new sample of OCD patients ($n=30$) and control subjects ($n=30$). The classifications for this new cohort were obtained by calculating subjects' individual expression values (*Step 2* above) against the group difference pattern extracted from the original sample ($n=144$).

In both validation studies, the predictive power of our classification tool was determined by calculating the sensitivity (i.e., the conditional probability that a case X was correctly classified as an OCD patient) and specificity (i.e., the conditional probability that a case X was correctly classified as a control

subject) values. Overall classification accuracy was then calculated as the average of these two values.

Analysis of sociodemographic and clinical variables

Potential differences in the sociodemographic characteristics of patient and control groups of both samples were assessed using Student's t and χ^2 tests. Sociodemographic and clinical values of the sample of newly recruited subjects were compared with those of the original sample by means of the one-sample t and χ^2 tests (see Tables 1 and 2).

We also conducted Pearson's correlation analyses between subjects' individual expression values and the continuous clinical and sociodemographic variables of interest, including subjects' age, duration of illness, cumulative use of serotonin reuptake inhibitors (SRI), comorbid anxious and depressive symptoms (Hamilton scores), and OC-symptom severity (Y-BOCS scores). Differences in individual expression values between subgroups of patients in terms of gender, major OC-symptom dimensions, previous SRI trials completed, and stable medication use at time of MRI, were assessed using Student's t test and one-way ANOVAs. The above analyses were performed using SPSS version 12.0.

Results

Table 1 summarizes the sociodemographic characteristics of both study samples. No significant differences were observed in any of the variables between the groups of OCD patients and control subjects in either of the samples. Similarly, sociodemographic characteristics of the newly recruited groups of OCD patients and control subjects did not significantly differ with respect to the original sample. Table 2 summarizes the major clinical characteristics of both groups of OCD patients. It can be seen that the new sample of patients differed significantly from the original cohort on 8 of the 17 clinical variables measured (see Table 2 for details).

The omnibus mean sum of squares test (described in *Step 1* above) indicated that the whole-brain pattern of anatomical differences between the original groups of control subjects and OCD patients was globally significant ($S=1.75$, $P<0.0001$). The most relevant features of this pattern are depicted in Fig. 2. As anticipated, the primary regions of difference between OCD patients and control subjects (i.e., gray matter volume increases and decreases) closely resemble those described in our previous study of these subjects (Pujol et al., 2004). To summarize here, significant volumetric decreases in OCD patients were observed in the medial wall of the prefrontal lobe, the posterior cingulate–precuneus region, the cerebellar tonsils, and the posterior insula bilaterally. Significant volumetric increases in OCD patients were observed primarily in subcortical regions, including ventral striatum bilaterally, the posterior thalamus, the anterior cerebellum, and the medial midbrain.

To test the accuracy of our subject classification pattern, we first carried out a cross-validation assessment on the original sample. From this analysis, we obtained a high rate of correct subject classification, expressing a sensitivity index of 91.7% and a specificity index of 94.4%. The overall rate of classification accuracy was 93.1% (see Fig. 3). This analysis was repeated including only the most extreme 30% of positive and negative

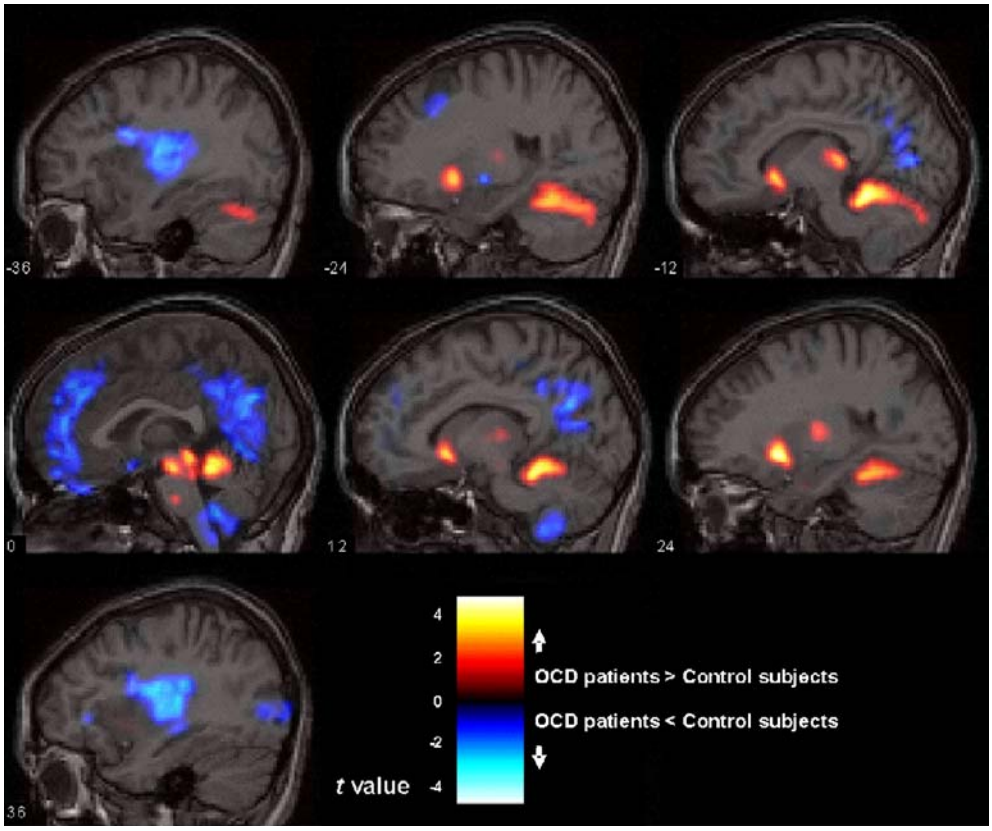

Fig. 2. Illustration of the whole-brain pattern of differences between groups. The numbers refer to the x coordinate in standard Montreal Neurological Institute (MNI) space.

voxel loadings of the *t* map. The result of this approach was a lower classification accuracy of 79.9%, with a sensitivity and specificity values of 75.0% and 84.7%.

In the subsequent, 'independent set of data' analysis, we then sought to assess the predictive power of the classification approach by repeating the same classification procedure on a new sample of OCD patients and control subjects. As shown in Fig. 4, the sensitivity and specificity values obtained from this assessment were somewhat lower, at 70% and 83.3%, respectively. Overall accuracy from this second analysis was 76.6%.

We also examined for potential associations between clinical and sociodemographic variables and individual expression values. Patients' overall severity of symptoms (total Y-BOCS score) showed a positive correlation with individual expression values, being this association slightly stronger in the new sample of OCD patients ($r=0.45$, $P<0.05$; see Fig. 5) than in the original sample ($r=0.23$, $P<0.05$). In a *post hoc* analysis, however, a statistical comparison of the strength of these correlation coefficients showed no significant differences in their magnitude ($z=1.11$, $P>0.05$).

Finally, although in the previous analyses we did not find any association between gender and individual expression values, we conducted an additional *post hoc* assessment to evaluate the influence of this relevant variable. Between-group difference patterns were again extracted, but for male and female subjects separately. Compared to results obtained from the whole sample, we obtained a better classification accuracy in these gender-specific cross-validation assessments (males: overall accuracy=98.8%, sensitivity=97.5%, specificity=100%; females: overall accuracy=100%, sensitivity=100%, specificity=100%). Accordingly, we also performed the same gender-specific classification on the new sample of OCD patients and control subjects. For male subjects, the sensitivity of this classification was reduced to 57.1% (9 out of 21 patients misclassified), while the specificity was higher, at 81.2% (3 out of 16 controls misclassified). Interestingly, 7 of the 9 OCD patients and 2 of the 3 controls misclassified by this analysis were also misclassified in the original 'independent set of data' assessment. Female OCD patients from the new sample were classified with a sensitivity of 77.8% (2 out of 9 patients misclassified, 1 patient also misclassified in the original analysis), while new female control subjects were classified with a specificity of 85.7% (2 out of 14 controls misclassified, both of them misclassified in the original analysis).

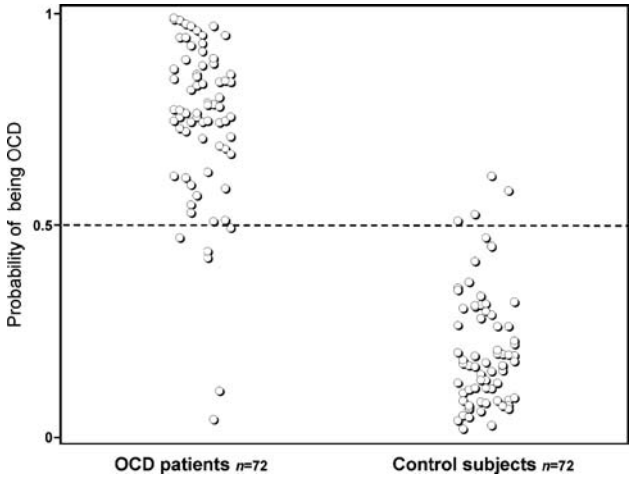

Fig. 3. Probability of being an OCD patient for the subjects of the original sample after cross-validation following the leave-one-out method.

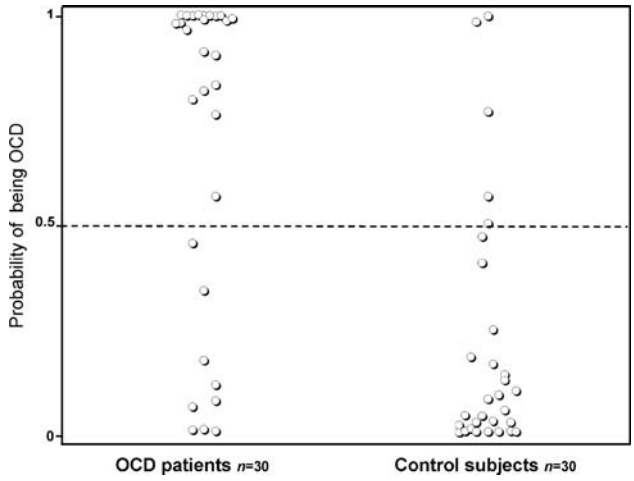

Fig. 4. Probability of being an OCD patient for the newly recruited subjects based on their expression values of the pattern extracted from the original sample.

Discussion

Magnetic resonance imaging studies employing voxel-wise analysis methods have reported significant structural brain alterations in OCD, including both increases and decreases of gray matter volume in distributed cortical and subcortical regions (Kim et al., 2001; Pujol et al., 2004; Valente et al., 2005). Methodologically, these analyses operate by collecting volumetric data from every single voxel in the brain, where group differences can be assessed throughout the entire cerebrum in a relatively automated fashion (Ashburner and Friston, 2000). Potential differences are then computed and a voxel-by-voxel statistical map of this comparison is generated (usually a Student's *t* test), where the highest (and lowest) values correspond to the brain

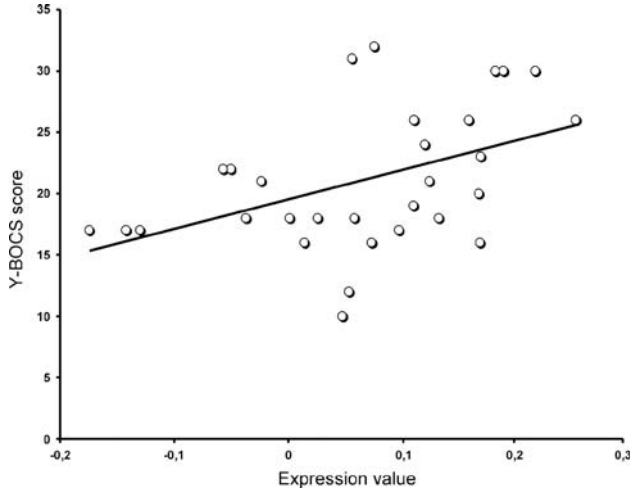

Fig. 5. Expression of the pattern (mean centered) plotted against the Y-BOCS score in the newly recruited group of OCD patients ($r=0.45$, $P=0.013$).

regions showing most alteration. However, these estimated volume values using voxel-wise assessments typically display a large overlap between groups of patients and control subjects (Davatzikos, 2004), making the identification of single OCD patients based on discrete voxel measurements rarely feasible.

In this study, contrary to the above notions, we tested the feasibility (and accuracy) of identifying OCD patients using a whole-brain pattern of anatomical alteration characterized by an optimized voxel-wise analysis of our large MRI series of patients and control subjects (Pujol et al., 2004). We calculated a between-group difference image (voxel-wise, *t* statistic) by comparing the gray matter volumes of an initial group of 72 OCD patients and 72 control subjects, and then used this resulting *t* map of structural alterations to obtain individual expression values for the gray matter volumes of each subject. We use the term "expression value" because this single metric represents the extent to which each individual subject expressed the global pattern of anatomical differences between groups, that is, the degree of "OCD-like" anatomical abnormality in a particular subject. These expression values may ultimately provide the psychiatrist with relevant biological information, especially when considering the relatively high level of accurate identifications that were generated in the validation assessments performed in the current study.

We validated the accuracy of our approach by performing two validation assessments with independent samples of OCD patients and control subjects. Our initial cross-validation assessment of the original sample yielded a 93.1% accuracy rating, which is encouraging, considering the large variability observed in the volumetric measures of psychiatric populations in structural neuroimaging studies. Interestingly, this accuracy was reduced when the pattern of alterations was limited to the most relevant voxels, suggesting that a whole-brain approach may be more optimal for the anatomical characterization of this disorder. However, because OCD is a clinical heterogeneous condition (Mataix-Cols et al., 2005), we also sought to assess how representative our classification approach was in a new set of OCD patients. To do so, we performed an 'independent set of data' test, which showed a reduced overall level of accuracy of individual classifications (76.6%) compared to the cross-validation assessment. This 16.5% decrease in accuracy between the two validations might be explained by the inherent statistical properties of each approach. The leave-one-out method is a very reliable estimator of the predictive power of a classifier, whereas the 'independent set of data' test has greater external and ecological validity, but depends critically on sample selection, yielding markedly different results with different sample selections (Chou and Zhang, 1995). In the clinical research, it is rarely possible to access a full population for random selection, and, typically, patients are recruited for research studies when they contact the health care system (Aitken et al., 2003). Although in our case the recruitment of OCD patients was made by the same psychiatrists using equivalent procedures, the clinical heterogeneity of the disorder and the recruitment of patients at two separate time points resulted in some differences in the clinical features of the samples (e.g., severity of the disorder, or history of depression, see Table 2). One parsimonious interpretation, therefore, is that the clinical differences between the original and the newly recruited sample may have led to a lower classification accuracy in the 'independent set of data' test. To increase sample homogeneity in future studies, analyses might be restricted to particular subsets of patients, such as severe patients, or patients without certain comorbidities that may affect brain anatomy (i.e., depression and other anxiety disorders). However, these approaches may ultimately reduce the generalizability of findings.

Gender-specific analyses were found to improve classification accuracy in the separate cross-validation assessments of male and female sub-groups. To some extent, this may be interpreted as a secondary validation of our classification method. These results also suggest a degree of sexual dimorphism in the anatomical alterations of OCD, in line with known gender effects that have been described in the clinical expression and genetic susceptibility to this disorder (Arnold et al., 2006; Bogetto et al., 1999; Lensi et al., 1996; Lochner et al., 2004). However, this result should be interpreted cautiously, as we did not observe any gender-specific anatomical alterations in our previous study of these patients (Pujol et al., 2004). Unlike the original study sample, the classification of new subjects did not benefit to the same extent when using such gender-specific patterns. Most of the subjects misclassified in the whole-sample analysis were also misclassified in the gender-specific analyses indicating that, in this case, misclassification was not attributable to gender differences.

Given the above results, it is important to emphasize that we do not consider that diagnosis of OCD can be made on the basis of a structural MRI examination. It seems that the accuracy of our classification approach will be inevitably influenced by different sources of patient heterogeneity. It is of special relevance, however, that the individual expression values of OCD patients (indicating relative severity of brain structural alterations), showed a significant positive correlation with patients' symptom severity. Although a greater expression of the pattern cannot be automatically associated with a more severe form of OCD, this suggests that underlying neuroanatomical alterations are indeed related to the overt clinical expression of the disorder. Further studies are needed to determine whether the joint use of anatomical and psychometric data may be useful in classifying particular subgroups of OCD patients, for example, based on primary symptom clusters as opposed to overall illness severity.

There are a number of considerations that may enhance the clinical relevance of our approach. For instance, if the progressive (Pujol et al., 2004), reversible (Gilbert et al., 2000), or reactive (Giedd et al., 1996) nature of some of the structural alterations of OCD was confirmed, pattern classifications could be used as an indicator of disease progression or stabilization. The potential clinical use of an approach such as ours would also be strengthened if a degree of discriminant validity with other psychiatric disorders was demonstrated. Similarly, if images acquired from different scanners could be analyzed in combination, multi-site clinical applications would be possible, facilitating the development of shared databases. However, site-specific image distortions also pose a major problem when seeking to make accurate comparisons of data from different scanners. Although some correction methods for these distortions (Jovicich et al., 2006), as well as some segmentation algorithms invariant to details of image acquisition (Fischl et al., 2002), have been proposed, a reliable method for performing multi-center VBM studies has not been developed yet. Nevertheless, observations from our laboratory using images of 9 OCD patients and 17 control subjects acquired from three different scanners (with identical parameters) suggest that multi-center classification accuracy of our method may be around 70%, i.e., less accurate than the 'independent set of data' test in the current study, but well above chance levels.

Our method follows the standard preprocessing steps implemented in VBM studies and uses a voxel-wise statistical mapping approach to calculate the pattern of between-group differences. Consequently, in this study, the nature of anatomical differences closely resembles the results of our previous VBM study of the original subject sample (Pujol et al., 2004). However, there are some minor differences between the two sets of findings, which are likely to be explained by the subtle differences in methodology described earlier. Additionally, our display of the whole-brain anatomical pattern of differences (Fig. 2) uses an arbitrary threshold of the most extreme 30% positive and negative voxel loadings, as opposed to a threshold dictated by voxel-wise statistics. As a result, certain regions, including the right posterior insula, the posterior cingulate–precuneus region, and the medial midbrain, now emerged as part of the difference pattern, whereas in our previous report they only showed a tendency towards significant alteration (Pujol et al., 2004).

Though largely restricted to neurological disorders, other approaches for patient classification with brain MRI have been developed with the intent of extending the clinical utility of neuroimaging studies. For example, the measurement of selected ROIs has been used to inform the diagnosis and clinical staging of neurodegenerative diseases (Laakso et al., 2000; Wolf et al., 2001), and VBM studies have characterized individual brains of neurological patients in relation to a population of reference (Gitelman et al., 2001; Mummery et al., 2000; Wilke et al., 2003; Woermann et al., 1999). However, in general, such classifications are likely to meet with less success when applied to psychiatric disorders, considering the high clinical heterogeneity that often exists between patients (Mataix-Cols et al., 2005). Similarly, in anatomical terms, structural brain abnormalities are also typically more variable and distributed in psychiatric groups, and thus, subtle alterations occurring in one individual patient may not be compelling when compared to a population of reference. Our notion is that the relevance of such subtle individual alterations could be enhanced if considered as part of an extended pattern of characteristic abnormality, which is variably expressed across subjects. In methodological terms, the use of high-resolution images with small smoothing kernels may be better suited for accurately characterizing such disease-associated patterns. Considering this, the relatively large slice thickness of images used in the current analysis may be one limitation of our study.

The use of whole-brain patterns of between-group differences for subject classification purposes has been previously reported, although, contrary to the present approach, within a multivariate statistical framework (Kawasaki et al., 2007; Kerrouche et al., 2006; Meyer-Lindenberg et al., 2001; Scarmeas et al., 2004). However, as discussed in the Materials and methods section, differences between univariate and multivariate approaches based on Singular Value Decomposition are only likely to arise when more than two study groups are involved (Worsley et al., 1997). Nevertheless, when combined with high-dimensional brain mapping techniques, multivariate statistics may offer the possibility of analyzing some morphometrical characteristics, such as shape, that have been reported to possess greater discriminative power than volumetric data (Csernansky et al., 1998; Posener et al., 2003). Davatzikos et al. (2005), for instance, used such an approach and a non-linear discrimination function to anatomically differentiate schizophrenia patients from control subjects, obtaining a classification ratio quite similar to the one reported here. However, in a practical sense, these methods require significantly more computational time and effort than the relatively straightforward approach described here.

In summary, we present a method for summarizing brain anatomical alterations of particular patients, demonstrated here in OCD, with regards to a reference pattern of abnormality that exists at the population level. While the application of this method has currently been restricted to MRI scans acquired with the same machine, the possibility of using multi-center image databases remains open and may further advance the general utility of this approach towards a valuable neuroimaging aid for patient management.

Acknowledgments

This study was supported in part by the Fondo de Investigación Sanitaria (Grants No. 00/0226 and PI020102), the Fundació La Marató TV3, and the Direcció General de Recerca de la Generalitat de Catalunya (Grants No. 1999SGR-328 and 2000XT-43). Dr. Harrison is supported by an NHMRC Training Award (I.D. 400420). We thank Gerald Fannon, PhD, for revising the manuscript.

References

Aitken, L., Gallagher, R., Madronio, C., 2003. Principles of recruitment and retention in clinical trials. Int. J. Nurs. Pract. 9, 338–346.

Arnold, P.D., Sicard, T., Burroughs, E., Richter, M.A., Kennedy, J.L., 2006. Glutamate transporter gene *SLC1A1* associated with obsessive–compulsive disorder. Arch. Gen. Psychiatry 63, 769–776.

Ashburner, J., Friston, K.J., 2000. Voxel-based morphometry—The methods. NeuroImage 11, 805–821.

Atmaca, M., Yildirim, B.H., Ozdemir, B.H., Aydin, B.A., Tezcan, A.E., Ozler, A.S., 2006. Volumetric MRI assessment of brain regions in patients with refractory obsessive–compulsive disorder. Prog. Neuropsychopharmacol. Biol. Psychiatry 30, 1051–1057.

Aylward, E.H., Harris, G.J., Hoehn-Saric, R., Barta, P.E., Machlin, S.R., Pearlson, G.D., 1996. Normal caudate nucleus in obsessive–compulsive disorder assessed by quantitative neuroimaging. Arch. Gen. Psychiatry 53, 577–584.

Bartha, R., Stein, M.B., Williamson, P.C., Drost, D.J., Neufeld, R.W., Carr, T.J., Canaran, G., Densmore, M., Anderson, G., Siddiqui, A.R., 1998. A short echo 1H spectroscopy and volumetric MRI study of the corpus striatum in patients with obsessive–compulsive disorder and comparison subjects. Am. J. Psychiatry 155, 1584–1591.

Bogetto, F., Venturello, S., Albert, U., Maina, G., Ravizza, L., 1999. Gender-related clinical differences in obsessive–compulsive disorder. Eur. Psychiatry 14, 434–441.

Choi, J.S., Kang, D.H., Kim, J.J., Ha, T.H., Lee, J.M., Youn, T., Kim, I.Y., Kim, S.I., Kwon, J.S., 2004. Left anterior subregion of orbitofrontal cortex volume reduction and impaired organizational strategies in obsessive–compulsive disorder. J. Psychiatr. Res. 38, 193–199.

Chou, K.C., Zhang, C.T., 1995. Prediction of protein structural classes. Crit. Rev. Biochem. Mol. Biol. 30, 275–349.

Csernansky, J.G., Joshi, S., Wang, L., Haller, J.W., Gado, M., Miller, J.P., Grenander, U., Miller, M.I., 1998. Hippocampal morphometry in schizophrenia by high dimensional brain mapping. Proc. Nat. Acad. Sci. U. S. A. 95, 11406–11411.

Davatzikos, C., 2004. Why voxel-based morphometric analysis should be used with great caution when characterizing group differences. NeuroImage 23, 17–20.

Davatzikos, C., Shen, D., Gur, R.C., Wu, X., Liu, D., Fan, Y., Hughett, P., Turetsky, B.I., Gur, R.E., 2005. Whole-brain morphometric study of schizophrenia revealing a spatially complex set of focal abnormalities. Arch. Gen. Psychiatry 62, 1218–1227.

Fischl, B., Salat, D.H., Busa, E., Albert, M., Dieterich, M., Haselgrove, C., van der Kouwe, A., Killiany, R., Kennedy, D., Klaveness, S., Montillo, A., Makris, N., Rosen, B., Dale, A.M., 2002. Whole brain segmentation: automated labeling of neuroanatomical structures in the human brain. Neuron 33, 341–355.

Friston, K.J., Ashburner, J., 2004. Generative and recognition models for neuroanatomy. NeuroImage 23, 21–24.

Giedd, J.N., Rapoport, J.L., Leonard, H.L., Richter, D., Swedo, S.E., 1996. Case study: acute basal ganglia enlargement and obsessive–compulsive symptoms in an adolescent boy. J. Am. Acad. Child Adolesc. Psych. 35, 913–915.

Giedd, J.N., Rapoport, J.L., Garvey, M.A., Perlmutter, S., Swedo, S.E., 2000. MRI assessment of children with obsessive–compulsive disorder or tics associated with streptococcal infection. Am. J. Psychiatry 157, 281–283.

Gilbert, A.R., Moore, G.J., Keshavan, M.S., Paulson, L.A., Narula, V., MacMaster, F.P., Stewart, C.M., Rosenberg, D.R., 2000. Decrease in thalamic volumes of pediatric patients with obsessive–compulsive disorder who are taking paroxetine. Arch. Gen. Psychiatry 57, 449–456.

Gitelman, D.R., Ashburner, J., Friston, K.J., Tyler, L.K., Price, C.J., 2001. Voxel-based morphometry of herpes simplex encephalitis. NeuroImage 13, 623–631.

Good, C.D., Johnsrude, I.S., Ashburner, J., Henson, R.N., Friston, K.J., Frackowiak, R.S., 2001. A voxel-based morphometric study of ageing in 465 normal adult human brains. NeuroImage 14, 21–36.

Jenike, M.A., Breiter, H.C., Baer, L., Kennedy, D.N., Savage, C.R., Olivares, M.J., O'Sullivan, R.L., Shera, D.M., Rauch, S.L., Keuthen, N., Rosen, B.R., Caviness, V.S., Filipek, P.A., 1996. Cerebral structural abnormalities in obsessive–compulsive disorder. A quantitative morphometric magnetic resonance imaging study. Arch. Gen. Psychiatry 53, 625–632.

Jovicich, J., Czanner, S., Greve, D., Haley, E., van der Kouwe, A., Gollub, R., Kennedy, D., Schmitt, F., Brown, G., Macfall, J., Fischl, B., Dale, A., 2006. Reliability in multi-site structural MRI studies: effects of gradient non-linearity correction on phantom and human data. NeuroImage 30, 436–443.

Kang, D.H., Kim, J.J., Choi, J.S., Kim, Y.I., Kim, C.W., Youn, T., Han, M.H., Chang, K.H., Kwon, J.S., 2004. Volumetric investigation of the frontal–subcortical circuitry in patients with obsessive–compulsive disorder. J. Neuropsychiatry Clin. Neurosci. 16, 342–349.

Kawasaki, Y., Suzuki, M., Kherif, F., Takahashi, T., Zhou, S.Y., Nakamura, K., Matsui, M., Sumiyoshi, T., Seto, H., Kurachi, M., 2007. Multivariate voxel-based morphometry successfully differentiates schizophrenia patients from healthy controls. NeuroImage 34, 235–242.

Kellner, C.H., Jolley, R.R., Holgate, R.C., Austin, L., Lydiard, R.B., Laraia, M., Ballenger, J.C., 1991. Brain MRI in obsessive–compulsive disorder. Psychiatry Res. 36, 45–49.

Kerrouche, N., Herholz, K., Mielke, R., Holthoff, V., Baron, J.C., 2006. (18) FDG PET in vascular dementia: differentiation from Alzheimer's disease using voxel-based multivariate analysis. J. Cereb. Blood Flow Metab. 26, 1213–1221.

Kim, J.J., Lee, M.C., Kim, J., Kim, I.Y., Kim, S.I., Han, M.H., Chang, K.H., Kwon, J.S., 2001. Grey matter abnormalities in obsessive–compulsive disorder: statistical parametric mapping of segmented magnetic resonance images. Br. J. Psychiatry 179, 330–334.

Kwon, J.S., Shin, Y.W., Kim, C.W., Kim, Y.I., Youn, T., Han, M.H., Chang, K.H., Kim, J.J., 2003. Similarity and disparity of obsessive–compulsive disorder and schizophrenia in MR volumetric abnormalities of the hippocampus–amygdala complex. J. Neurol. Neurosurg. Psychiatry 74, 962–964.

Laakso, M.P., Hallikainen, M., Hanninen, T., Partanen, K., Soininen, H., 2000. Diagnosis of Alzheimer's disease: MRI of the hippocampus vs delayed recall. Neuropsychologia 38, 579–584.

Lensi, P., Cassano, G.B., Correddu, G., Ravagli, S., Kunovac, J.L., Akiskal, H.S., 1996. Obsessive–compulsive disorder. Familial–developmental history, symptomatology, comorbidity and course with special reference to gender-related differences. Br. J. Psychiatry 169, 101–107.

Lochner, C., Hemmings, S.M., Kinnear, C.J., Moolman-Smook, J.C., Corfield, V.A., Knowles, J.A., Niehaus, D.J., Stein, D.J., 2004. Gender in obsessive–compulsive disorder: clinical and genetic findings. Eur. Neuropsychopharmacol. 14, 105–113.

Mataix-Cols, D., Rauch, S.L., Manzo, P.A., Jenike, M.A., Baer, L., 1999. Use of factor-analyzed symptom dimensions to predict outcome with serotonin reuptake inhibitors and placebo in the treatment of obsessive–compulsive disorder. Am. J. Psychiatry 156, 1409–1416.

Mataix-Cols, D., Rosario-Campos, M.C., Leckman, J.F., 2005. A multidimensional model of obsessive–compulsive disorder. Am. J. Psychiatry 162, 228–238.

Meyer-Lindenberg, A., Poline, J.B., Kohn, P.D., Holt, J.L., Egan, M.F., Weinberger, D.R., Berman, K.F., 2001. Evidence for abnormal cortical functional connectivity during working memory in schizophrenia. Am. J. Psychiatry 158, 1809–1817.

Mummery, C.J., Patterson, K., Price, C.J., Ashburner, J., Frackowiak, R.S., Hodges, J.R., 2000. A voxel-based morphometry study of semantic dementia: relationship between temporal lobe atrophy and semantic memory. Ann. Neurol. 47, 36–45.

Posener, J.A., Wang, L., Price, J.L., Gado, M.H., Province, M.A., Miller, M.I., Babb, C.M., Csernansky, J.G., 2003. High-dimensional mapping of the hippocampus in depression. Am. J. Psychiatry 160, 83–89.

Pujol, J., Soriano-Mas, C., Alonso, P., Cardoner, N., Menchon, J.M., Deus, J., Vallejo, J., 2004. Mapping structural brain alterations in obsessive–compulsive disorder. Arch. Gen. Psychiatry 61, 720–730.

Rauch, S.L., Baxter Jr., L.R., 1998. Neuroimaging in obsessive–compulsive disorder and related disorders. In: Jenike, M.A., Baer, L., Minichiello, W.E. (Eds.), Obsessive–compulsive Disorder: Practical Management. Mosby-Year Book Inc., St. Louis, pp. 289–317.

Riffkin, J., Yucel, M., Maruff, P., Wood, S.J., Soulsby, B., Olver, J., Kyrios, M., Velakoulis, D., Pantelis, C., 2005. A manual and automated MRI study of anterior cingulate and orbito-frontal cortices, and caudate nucleus in obsessive–compulsive disorder: comparison with healthy controls and patients with schizophrenia. Psychiatry Res. 138, 99–113.

Robinson, D., Wu, H., Munne, R.A., Ashtari, M., Alvir, J.M., Lerner, G., Koreen, A., Cole, K., Bogerts, B., 1995. Reduced caudate nucleus volume in obsessive–compulsive disorder. Arch. Gen. Psychiatry 52, 393–398.

Rosenberg, D.R., Keshavan, M.S., O'Hearn, K.M., Dick, E.L., Bagwell, W.W., Seymour, A.B., Montrose, D.M., Pierri, J.N., Birmaher, B., 1997. Frontostriatal measurement in treatment-naive children with obsessive–compulsive disorder. Arch. Gen. Psychiatry 54, 824–830.

Salmond, C.H., Ashburner, J., Vargha-Khadem, F., Connelly, A., Gadian, D.G., Friston, K.J., 2002. Distributional assumptions in voxel-based morphometry. NeuroImage 17, 1027–1030.

Saxena, S., Brody, A.L., Schwartz, J.M., Baxter, L.R., 1998. Neuroimaging and frontal–subcortical circuitry in obsessive–compulsive disorder. Br. J. Psychiatr., Suppl. 35, 26–37.

Scarmeas, N., Habeck, C.G., Zarahn, E., Anderson, K.E., Park, A., Hilton, J., Pelton, G.H., Tabert, M.H., Honig, L.S., Moeller, J.R., Devanand, D.P., Stern, Y., 2004. Covariance PET patterns in early Alzheimer's disease and subjects with cognitive impairment but no dementia: utility in group discrimination and correlations with functional performance. NeuroImage 23, 35–45.

Scarone, S., Colombo, C., Livian, S., Abbruzzese, M., Ronchi, P., Locatelli, M., Scotti, G., Smeraldi, E., 1992. Increased right caudate nucleus size in obsessive–compulsive disorder: detection with magnetic resonance imaging. Psychiatry Res. 45, 115–121.

Stein, D.J., Coetzer, R., Lee, M., Davids, B., Bouwer, C., 1997. Magnetic resonance brain imaging in women with obsessive–compulsive disorder and trichotillomania. Psychiatry Res. 74, 177–182.

Szeszko, P.R., Robinson, D., Alvir, J.M., Bilder, R.M., Lencz, T., Ashtari, M., Wu, H., Bogerts, B., 1999. Orbital frontal and amygdala volume reductions in obsessive–compulsive disorder. Arch. Gen. Psychiatry 56, 913–919.

Szeszko, P.R., MacMillan, S., McMeniman, M., Chen, S., Baribault, K., Lim, K.O., Ivey, J., Rose, M., Banerjee, S.P., Bhandari, R., Moore, G.J.,

Rosenberg, D.R., 2004a. Brain structural abnormalities in psychotropic drug-naive pediatric patients with obsessive–compulsive disorder. Am. J. Psychiatry 161, 1049–1056.

Szeszko, P.R., MacMillan, S., McMeniman, M., Lorch, E., Madden, R., Ivey, J., Banerjee, S.P., Moore, G.J., Rosenberg, D.R., 2004b. Amygdala volume reductions in pediatric patients with obsessive–compulsive disorder treated with paroxetine: preliminary findings. Neuropsychopharmacology 29, 826–832.

Valente Jr., A.A., Miguel, E.C., Castro, C.C., Amaro Jr., E., Duran, F.L., Buchpiguel, C.A., Chitnis, X., McGuire, P.K., Busatto, G.F., 2005. Regional gray matter abnormalities in obsessive–compulsive disorder: a voxel-based morphometry study. Biol. Psychiatry 58, 479–487.

Wilke, M., Kassubek, J., Ziyeh, S., Schulze-Bonhage, A., Huppertz, H.J., 2003. Automated detection of gray matter malformations using optimized voxel-based morphometry: a systematic approach. NeuroImage 20, 330–343.

Woermann, F.G., Free, S.L., Koepp, M.J., Sisodiya, S.M., Duncan, J.S., 1999. Abnormal cerebral structure in juvenile myoclonic epilepsy demonstrated with voxel-based analysis of MRI. Brain 122, 2101–2108.

Wolf, H., Grunwald, M., Kruggel, F., Riedel-Heller, S.G., Angerhofer, S., Hojjatoleslami, A., Hensel, A., Arendt, T., Gertz, H., 2001. Hippocampal volume discriminates between normal cognition; questionable and mild dementia in the elderly. Neurobiol. Aging 22, 177–186.

Worsley, K.J., Poline, J.B., Vandal, A.C., Friston, K.J., 1995. Tests for distributed, nonfocal brain activations. NeuroImage 2, 183–194.

Worsley, K.J., Poline, J.B., Friston, K.J., Evans, A.C., 1997. Characterizing the response of PET and fMRI data using multivariate linear models. NeuroImage 6, 305–319.